Impact of the Human Motion on the Variance of the Received Signal Strength of Wireless Links

Conference Paper · September 2011

CITATIONS
9

READS
65

3 authors, including:

Moustafa Youssef
Egypt-Japan University of Science and Technology
219 PUBLICATIONS **5,345** CITATIONS

SEE PROFILE

Impact of the Human Motion on the Variance of the Received Signal Strength of Wireless Links

Kareem El-Kafrawy*, Moustafa Youssef†, Amr El-Keyi*
* Wireless Intelligent Networks Center (WINC), Nile University, Egypt
Email: {kareem.elkafrawy, aelkeyi}@nileu.edu.eg
† Alexandria University and EJUST, Egypt
Email: moustafa.youssef@ejust.edu.eg

***Abstract*—Human motion has strong impact on the received signal strength (RSS) of indoor wireless links that can be exploited for variance-based device-free positioning. In this paper, we investigate the effect of human motion on the variance of the RSS of wireless local area networks (WLAN) operating at 2.4 GHz. Using measurements, the RSS variance for human in-place motion is determined as a function of the human position in a corridor setting. We provide ray tracing and empirical models to capture this effect. The accuracy of the different models is compared under different scenarios. Furthermore, we investigate the effect of having multiple-entities in the same area of interest on the RSS variance and provide models for it.**

I. Introduction

Indoor device-free positioning, where an entity is tracked without carrying any device based on its effect on the wireless signal, has received increasing attention recently with many promising applications [1]–[4]. These applications include intruder detection and tracking, border protection, and building automation. While other systems, such as infrared-based systems and video cameras, have been used extensively for such purposes, these systems are quite costly, only operate in the presence of light and/or in limited areas, and provides limited tracking capabilities.

The activity of people within the vicinity of a wireless network has a considerable effect on the wireless links. This effect was used for device-free localization in WLANs [1], where an offline calibration phase was used to construct the radiomap: RSS at the monitoring points (MPs) due to the transmission of the access points (APs), as a function of the human position. In the online phase, the RSS at the MPs is used to estimate the person's position by comparing the RSS to the radiomap. The offline calibration phase requires extensive measurements, which consume a lot of time and effort. Using models for the human impact on the RSS can make these systems easier to deploy and less costly.

The Radio Tomographic Imaging (RTI) concept was introduced in [5], where wireless sensor networks are placed around the area of interest and each node transmits in turn. The RSS from each node is monitored at all other nodes and sent to a central node for processing. An image of the entity moving inside the area of interest is drawn using the RSS attenuation caused when cutting the LOS for some of the node pairs. Variance of the RSS due to human motion was used in [3] for through-wall human tracking. The system works just like RTI, only using the variance instead of the RSS. A very simple model is used for the human motion impact on the RSS variance, a binary model that assigns a non-zero weight only if the human is cutting the LOS. Adding a more realistic human motion model would increase the localization accuracy of such a system.

Studying the effect of people on the indoor wireless link is very important for the design for RF-based device-free positioning systems. It is needed to modify the current systems to higher accuracy or easier deployment, as seen in the above examples. It is also needed to provide a deeper understanding of the problem, which can lead to designing better systems. In the literature, there have been two approaches for determining the human impact on indoor links. On one hand, measurements were conducted on real channels with moving humans. Measurements were conducted for indoor channels with random motion pattern in [6], while predefined human motion paths were studied in [7] and [8]. These measurements however target the channel statistics, and do not relate the RSS to the human position, hence cannot be used in positioning applications. On the other hand, other work in the literature focused on the human body impact on incident waves. The human radar cross section (RCS) was determined in [9], and was used in [10]. RCS however is limited to only a single, static posture of the person, and is also very complicated to include in a practical model. The human body was modeled as a metallic cylinder in [11]. However, measurements validating the use of these models in real life scenarios have not been carried out. The effect of moving people along the LOS has been modeled using an extension of the well-known knife edge diffraction in [12]. However, this model is limited to the LOS case only.

In this paper, we attempt to determine the impact of human motion on the RSS variance of a wireless link, as a function of the person's position. Position dependence is realized using in-place motion. We perform measurements over different AP-MP set-ups in a corridor setting, and develop models to capture this effect. We present a ray-tracing-based model, where we assume that rays passing by the moving human change their phase randomly. The RSS variance is obtained by phase perturbation of the affected rays. We also present the ellipsoid model: an empirical model where the variance depends on the person's location relative to the AP-MP LOS. Both models are

978-1-4577-1348-4/11/$26.00 ©2011 IEEE

compared against measurements. We additionally investigate the effect of multiple moving persons on the RSS variance and provide models for this effect.

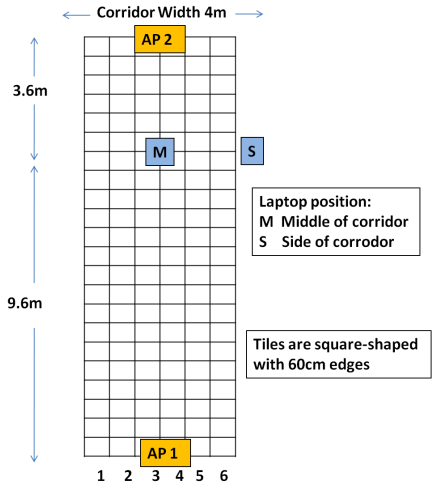

Fig. 1. Corridor setting layout

II. Single Entity Models

In this section, we examine the impact of the motion of a single person on the variance of the RSS. We begin the section by describing the measurement setup. We then provide different models to fit the measured data, and compare the performance of these models. We start with the ray tracing model, followed by the empirical ellipsoid model, and then a hybrid model combining both the ray tracing and ellipsoid models.

A. Measurement Setup

In order to investigate the human motion impact on the RSS variance as a function of location, we divide the area of interest into small tiles. At each measurement point the human walks in-place at the center of the tile. Readings were taken in a corridor setting using 2 APs, with the layout shown in Fig. 1, for square-shaped tiles having edges of length 60 cm. APs are ceiling-mounted at a height of 278 cm. Cisco Aironet APs are used, at a frequency of 2.45 GHz using 802.11g. The MP is a Dell laptop which is laid on a wooden table at a height of 75 cm, with a D-Link AirPlus G+ wireless card, model number DWL-G650+. A total of 300 RSS samples are captured at each point, at a sampling rate of 10 samples per second.

In the following subsections, we provide different models for the effect of the human motion on the variance of the RSS. Physically, the human motion affects the RSS by either shadowing and diffraction, or by scattering. The scattered components continuously change in magnitude and phase, as the human motion causes different areas of the human body to scatter the incident wave at every time instant. The change in magnitude and phase of the scattered wave is due to the irregular RCS of the human body [9], [10].

B. Three-dimensional Ray tracing Model

We assume that that the presence of the human near a propagating ray causes a change in the phase of that ray, as suggested in [3]. A ray is affected by the presence of the human if it passes in the volume above the tile in which the person is moving. We extend this model to include multipath components in addition to the LOS component. In order to simulate the variance in the RSS, a loop runs where we perturb the phase of each affected ray. The phase of the perturbed ray takes each time a certain value as a sample of the whole angular spectrum, e.g., we take 20 samples over the 0 to 2π range for each ray. In the case of multiple affected rays, nested loops are used. We then calculate the variance of the RSS from the RSS values caused by different ray phases. Fig. 2 compares the standard deviation of the RSS obtained using measurements and that calculated from the above ray tracing model. We can see from Fig. 2 that the ray tracing model has two main shortcomings. The first is that the variance predicted by the model in most of the corridor area is lower than the measured variance. The second drawback is that the variance in the areas where a reflection ray passes is much higher in the model compared to measurements.

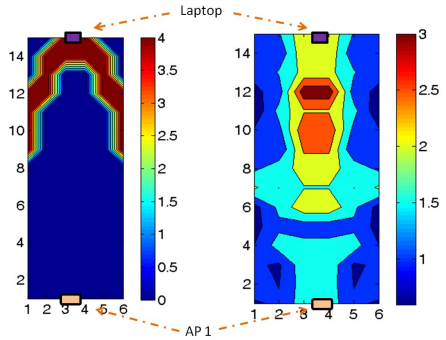

Fig. 2. RSS standard deviation (in dB) for AP 1 and MP at the middle, against position (tile numbers). Ray tracing model (left) and measurements (right).

C. Ray Tracing Model with Attenuation and Scattering

In order to address the shortcomings of the ray tracing-based variance simulator, we consider the attenuation and scattering caused by the presence of the human. We add a scattering component at the locations where the human presence does not affect the LOS- or multipath-induced rays. Since the exact orientation of the person changes due to motion, the reflection co-efficient of the scattered component is not a constant, rather it changes with motion. Hence, we will use a range of reflection coefficients of 0.1 to 0.7, representative values of the human RCS [10], [13]. In each sample, a single value of the reflection coefficient is used. We also add an attenuation factor for the multipath components cut by the person. Results are shown in Fig. 3 for AP1 and MP in the middle.

We can see from Fig. 3 that the ray tracing model with scattering and attenuation is still unable to capture the effect of the scattering with its proper weight, where a moving human near the LOS has a very strong effect and as we move away from the LOS the effect diminishes.

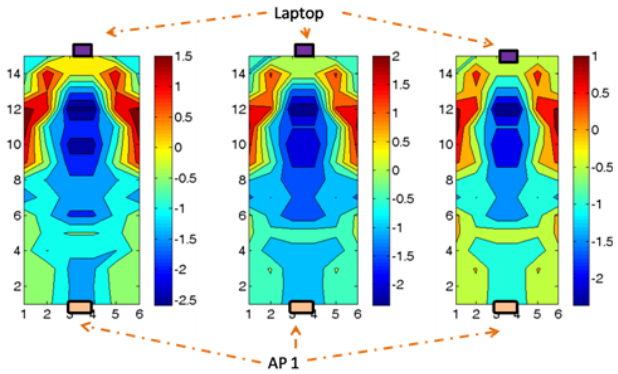

Fig. 3. Difference between simulated and measured RSS standard deviation (in dB) for: Attenuation = 0.5 and Scattering range 0.1 to 0.7 (left), Attenuation = 0.5 and Scattering range 0.3 to 0.8 (middle), Attenuation = 0.2 and Scattering range 0.3 to 0.8 (right)

D. Ellipsoid Model

The ellipsoid model was mentioned in [3], but it was not validated nor compared to measurements. We define a 3-dimensional ellipsoid associated with the LOS between the AP and the MP. The AP and the MP are located at the two foci of the ellipsoid, whose minor axes are equal and denoted as b. Fig. 4 is a 2D cut of the ellipsoid, illustrating the AP and MP placement. The major axis a is determined as a function of the minor axes b and the AP-MP distance $2f$ as in equation 1.

$$a = \sqrt{(2f)^2 + b^2} \tag{1}$$

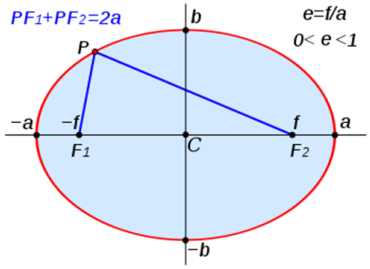

Fig. 4. Illustration of the ellipsoid model

We provide an empirical model for the RSS standard deviation σ as a function of the minor axes length b of the smallest ellipsoid cut by the human. Let σ_i denote the variance of the RSS due to the presence of the human at point i where $i = 1, \ldots, N$ and N is the number of points used for calibrating the model. For each of the N points where the human walks in-place, we calculate the standard deviation of the measured RSS values when the human is present at this point. Let b_i denote the length of the minor axis of the ellipsoid passing through point i. We will investigate the use of the following models for the dependence of σ_i on b_i.

1) Linear dependence model

$$\sigma_i = \alpha_1 b_i + \alpha_2 \qquad \forall i = 1, \ldots, N. \tag{2}$$

where the parameters α_1 and α_2 are estimated by fitting the measured values of the standard deviation. We can write the above equations in matrix form as

$$\boldsymbol{\sigma} = \boldsymbol{A}_L \boldsymbol{\alpha} \tag{3}$$

where $\boldsymbol{\sigma} = [\sigma_1, \ldots, \sigma_N]^T$, $\boldsymbol{\alpha} = [\alpha_1, \alpha_2]^T$, and

$$A_L = \begin{bmatrix} b_1 & 1 \\ \vdots & 1 \\ b_N & 1 \end{bmatrix}. \tag{4}$$

2) Quadratic dependence model

$$\sigma_i = \alpha_1 b_i^2 + \alpha_2 b_2^2 + \alpha_3 \tag{5}$$

where the parameters α_1, α_2, and α_3 are estimated from the measurements. We can also write the above equation in matrix form as

$$\boldsymbol{\sigma} = \boldsymbol{A}_Q \boldsymbol{\alpha} \tag{6}$$

where $\boldsymbol{\sigma} = [\sigma_1, \ldots, \sigma_N]^T$, $\boldsymbol{\alpha} = [\alpha_1, \alpha_2, \alpha_3]^T$, and

$$A_Q = \begin{bmatrix} b_1^2 & b_1 & 1 \\ \vdots & \vdots & 1 \\ b_N^2 & b_N & 1 \end{bmatrix}. \tag{7}$$

3) Exponential dependence model

$$\sigma_i = \alpha_1 e^{\alpha_2 * b_i} \tag{8}$$

Taking the logarithm of the above equation, we can write the matrix equation

$$\boldsymbol{y} = \boldsymbol{A}_L \boldsymbol{\alpha} \tag{9}$$

where $\boldsymbol{y} = [\log(\sigma_1), \ldots, \log(\sigma_N)]^T$, $\boldsymbol{\alpha} = [\alpha_1, \alpha_2]^T$.

The above three dependence models in (3), (6), and (9) are linear in the coefficient vector $\boldsymbol{\alpha}$ and can be written in the form $\boldsymbol{z} = \boldsymbol{A}\boldsymbol{\alpha}$. The coefficient vector $\boldsymbol{\alpha}$ can be estimated using least squares [14] as

$$\boldsymbol{\alpha} = (\boldsymbol{A}^T \boldsymbol{A})^{-1} \boldsymbol{A}^T \boldsymbol{z}. \tag{10}$$

E. Hybrid Ellipsoid Model

The ellipsoid model presented in Section II-D does not take into account the effect of the presence of the human on the multipath-induced components of the received wireless signals. In the Hybrid Ellipsoid model, we provide an empirical model for the RSS standard deviation σ as a function of the ellipsoid minor axes length b and the multipath components. Let us define the binary variable m_i where $m_i = 1$ when one or more multipath components are cut due to the presence of the human at point i. On the other hand $m_i = 0$ when the human presence at point i does not lead to cutting any multipath component. The above linear and quadratic models can be augmented to include the effect of cutting the multipath components as follows

1) Hybrid linear model

$$\sigma_i = \alpha_1 b_i + \alpha_2 m_i + \alpha_3 \qquad \forall i = 1, \ldots, N. \tag{11}$$

2) Hybrid quadratic model

$$\sigma_i = \alpha_1 b_i^2 + \alpha_2 b_2^2 + \alpha_3 m_i + \alpha_4 \tag{12}$$

The parameter vector $\boldsymbol{\alpha}$ can also be estimated using least squares from the measured variance of the RSS at the N grid calibration points.

F. Results

The parameters for each model are fitted using least squares and measurements of AP1 and MP in the middle setup, and then these parameters are used for all other measurement setups. For each of the models presented in this section, the RMS difference between the measured RSS and the predicted RSS are shown in Table I. We fit the parameters of the model using measurement data of AP1 and MP at the side setup. We can see that the RMS difference between measurements and the models is small for all models, and that the performance of all models is very close. The hybrid model does not bring performance improvement. The linear dependence model seems the most suitable model, since it is the simplest, with similar performance to more complicated models. The difference between the ellipsoid model and the measured RSS standard deviation for the AP1 and MP in the middle is shown in Fig. 5. We can see from the figure that the ellipsoid model is closer to the measured data than the ray tracing model.

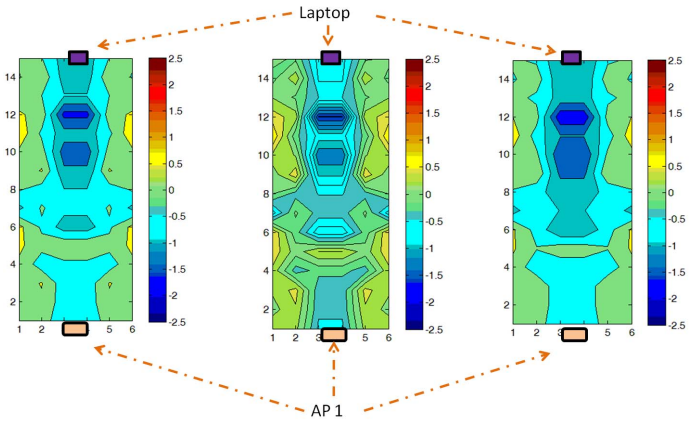

Fig. 5. Difference between RSS variance predicted by ellipsoid model and measured RSS variance (in dB), for linear dependence (left), quadratic dependence (middle), and exponential dependence (right)

III. Multiple-Entity Model

In this section, we characterize the effect of multiple moving persons on the variance of the RSS. We use the same corridor setup described in Section II-A, using AP1 and the MP in the middle. In this experiment, there are 2 persons who move in place. There are 4 rounds with 12 measurements in each round. As illustrated in Fig. 6, for round i, person 2 moves in-place in yellow-shaped (light) tile i, and 12 measurements are taken for person 1 moving in-place at one of the red-shaded (dark) tiles for each measurement.

From Fig. 7, we can notice that two moving persons results in higher RSS variance, except when one of the persons is very close to the LOS. In this case the RSS variance is very similar to the case when there is only one person. Let $\sigma_i^{(k)}$

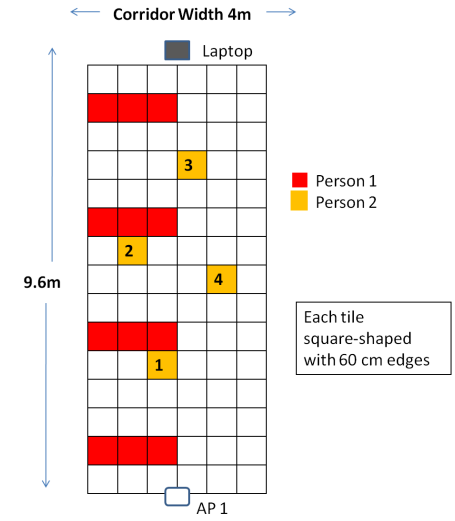

Fig. 6. Corridor experiment set-up for multi-person effect on RSS variance

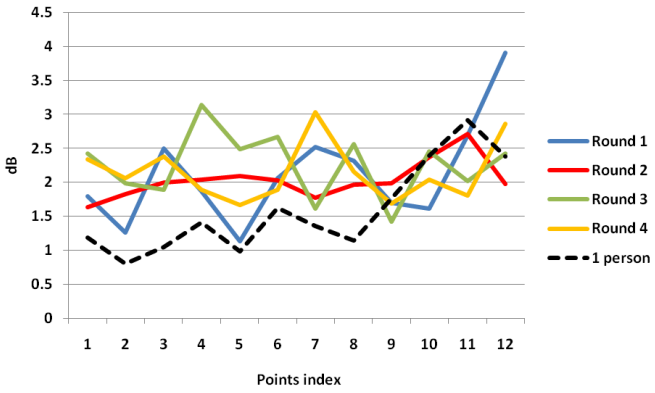

Fig. 7. Measurements results for multi-person effect on RSS variance

denote the variance of the RSS due to the presence of person k at location i where $\sigma_i^{(k)}$ is given by the linear model in equation (2). Let σ_{ij} denote the variance of the RSS due to the presence of the first person at location i and the second at location j. The following two models can be used to capture the effect of the presence of the two persons on the variance of the RSS

- Dominant effect model

$$\sigma_{ij} = \max\{\sigma_i^{(1)}, \sigma_j^{(2)}\} \tag{13}$$

- Additive model

$$\sigma_{ij} = \sigma_i^{(1)} + c\sigma_j^{(2)}. \tag{14}$$

where c is a scaling factor given by

$$c = \frac{\sum_{i=1}^{12} \sigma_i^{(1)} - \sigma_j^{(2)}}{12} \tag{15}$$

The results of these models are given in Table II. Fig. 8 illustrates the performance of different models for round 1. We can see from the results that the proposed models are

TABLE I
RMS DIFFERENCE BETWEEN MODEL AND MEASURED RSS STANDARD DEVIATION FOR DIFFERENT SCENARIOS USING DIFFERENT FIT APPROACHES

Scenario	Linear	Hybrid linear	Quadratic	Hybrid Quadratic	Exponential
AP1 middle	0.53	0.54	0.50	0.51	0.59
AP1 side	0.65	0.65	0.64	0.64	0.66
AP2 middle	1.13	1.12	1.15	1.15	1.23
AP2 side	0.90	0.90	0.89	0.90	0.91
Average	0.71	0.71	0.70	0.70	0.75

TABLE II
RMS DIFFERENCE BETWEEN MODEL AND MEASURED RSS STANDARD DEVIATION FOR 2 MOVING PERSONS, FOR DIFFERENT MODELS. THE RESULTS ARE PRESENTED FOR DIFFERENT POSITIONS OF PERSON 2, AS DESCRIBED IN FIG. 6

Models	Position 1	Position 2	Position 3	Position 4
Person 1 only	0.79	0.59	0.98	0.79
Person 2 only	0.74	0.37	0.47	0.55
Additive model	0.57	0.35	0.71	0.55
Dominant model	0.67	0.26	0.47	0.51

reasonably accurate, with the additive model better at following the measured trend. The dominant effect model however has the lowest RMS difference compared to measurements, as it generally captures the average values of the measured variance.

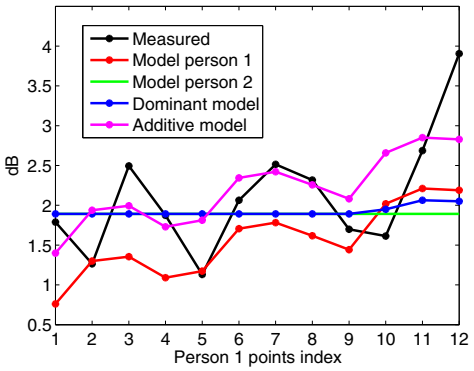

Fig. 8. Measurements and models for the RSS standard deviation due to motion of 2 persons against the position index for person 1, for person 2 moving at position 1

IV. CONCLUSION

We have investigated the effect of human motion on the RSS variance of wireless links. We have presented measurement results for RSS variance against position for in-place motion of humans for a corridor setting under different AP-MP placements. We have provided models that fit these measurement results. First, we presented the ray-tracing-based model which builds on the assumption that the moving human randomly changes the phase of the passing rays. We have also presented the ellipsoid model where the variance depends on the relative location of the human with respect to the AP-MP LOS component. We have compared these models to the measurements, and found that the ellipsoid model achieves the best performance. We have also presented an empirical model for the multiple moving entities case.

Future work in this area includes taking measurements under different settings and buildings to validate the measurement results presented here. It is also very important to investigate physical models that can fit any AP-MP placement and any building layout. More investigation needs to be pursued for the case of multiple-moving entities to obtain more accurate empirical models.

V. ACKNOWLEDGEMENTS

This work is supported in part by the Egyptian Science and Technology Development Fund (STDF).

REFERENCES

[1] M. Youssef, M. Mah, and A. Agrawala. Challenges: device-free passive localization for wireless environments. In *MobiCom '07: Proceedings of the 13th annual ACM international conference on Mobile computing and networking*, 2007.

[2] M. Seifeldin and M. Youssef. A deterministic large-scale device-free passive localization system for wireless environments. In *PETRA '10: Proceedings of the 3rd International Conference on PErvasive Technologies Related to Assistive Environments*, 2010.

[3] J. Wilson and N. Patwari. See through walls: Motion tracking using variance-based radio tomography networks. *IEEE Transactions on Mobile Computing*, accepted.

[4] D. Zhang, J. Ma, Q. Chen, and L. M. Ni. An RF-based system for tracking transceiver-free objects. In *IEEE International Conference on Pervasive Computing and Communications (Percom)*, March 2007.

[5] J. Wilson and N. Patwari. Radio tomographic imaging with wireless networks. *IEEE Transactions on Mobile Computing*, accepted.

[6] I. Kashiwagi, T. Taga, and T. Imai. Time-varying path-shadowing model for indoor populated environments. *IEEE Transactions on Vehicular Technology*, 59(1):16–28, January 2010.

[7] A. Rahim, S. Zeisberg, M.L. Fernandez, and A. Finger. Impact of people movement on received signal in fixed indoor radio communications. In *IEEE International Symposium on Personal, Indoor and Mobile Radio Communications (PIMRC)*, September 2006.

[8] H. Hashemi, M. McGuire, T. Vlasschaert, and D. Tholl. Measurements and modeling of temporal variations of the indoor radio propagation channel. *IEEE Transactions on Vehicular Technology*, 43(3):733–737, August 1994.

[9] N. Yamada, Y. Tanaka, and K. Nishikawa. Radar cross section for pedestrian in 76 GHz band. In *European Microwave Conference*, October 2005.

[10] K. I. Ziri-Castro, W. G. Scanlon, and N. E. Evans. Prediction of variation in MIMO channel capacity for the populated indoor environment using a radar cross-section-based pedestrian model. *IEEE Transactions on Antennas and Propagation*, 4(3):1186–1194, May 2005.

[11] M. Ghaddar, L. Talibi, T.A. Denidni, and A. Sebak. A conducting cylinder modeling human body presence in indoor propagation channel. *IEEE Transactions on Antennas and Propagation*, 55(11):3099–3103, November 2007.

[12] M. Varney, Z. Ji, M. Takai, and R. Bagrodia. Modeling environmental mobility and its effect on the network protocol stack. In *Wireless Communication and Networking Conference (WCNC)*, April 2006.

[13] F. Villanese, W. G. Scanlin, and N. E. Evans. Statistical characteristics of pedestrian-induced fading for a narrowband 2.45 GHz indoor channel. In *Vehicular Technology Conference (VTC)*, 2000.

[14] S.M. Kay. *Fundamentals of Statistical Signal Processing: Estimation Theory*. Prentice Hall, 1993.